JOC The Journal of Organic Chemistry

Article

pubs.acs.org/joc

Computational Investigations on Base-Catalyzed Diaryl Ether Formation

Gavin O. Jones,[†] Ali Al Somaa,[‡] Jeannette M. O'Brien,[†] Hassan Albishi,[‡] Hamid A. Al-Megren,[‡] Abdullah M. Alabdulrahman,[‡] Fares D. Alsewailem,[‡] James L. Hedrick,[†] Julia E. Rice,[†] and Hans W. Horn*[,†]

[†]IBM Almaden Research Center, 650 Harry Road, San Jose, California 95120, United States

[‡]King Abdulaziz City for Science and Technology, P.O. Box 6086, Riyadh 11442, Saudi Arabia

Supporting Information

ABSTRACT: We report investigations with the dispersion-corrected B3LYP density functional method on mechanisms and energetics for reactions of group I metal phenoxides with halobenzenes as models for polyether formation. Calculated barriers for ether formation from *para*-substituted fluorobenzenes are well correlated with the electron-donating or -withdrawing properties of the substituent at the *para* position. These trends have also been explained with the distortion/interaction energy theory model which show that the major component of the activation energy is the energy required to distort the arylfluoride reactant into the geometry that it adopts at the transition state. Resonance-stabilized aryl anion intermediates (Meisenheimer complexes) are predicted to be energetically disfavored in reactions involving fluorobenzenes with a single electron-withdrawing group at the *para* position of the arene, but are formed when the fluorobenzenes are very electron-deficient, or when chelating substituents at the *ortho* position of the aryl ring are capable of binding with the metal cation, or both. Our results suggest that the presence of the metal cation does not increase the rate of reaction, but plays an important role in these reactions by binding the fluoride or nitrite leaving group and facilitating displacement. We have found that the barrier to reaction decreases as the size of the metal cation increases among a series of group I metal phenoxides due to the fact that the phenoxide becomes less distorted in the transition state as the size of the metal increases.

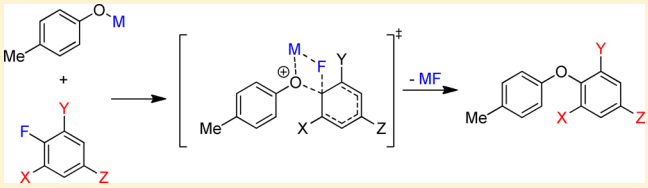

INTRODUCTION

Poly(aryl ethers) are an important class of organic materials that are commonly used in a variety of settings requiring the use of materials with thermo-oxidative[1] and radiation stability.[2] Such properties have rendered these materials useful as high-vacuum fluids, fluids in diffusion pumps, high temperature lubricants and greases,[3] and engineering thermoplastics.[4]

Poly(aryl ethers) are typically prepared by alkoxide-catalyzed step growth polymerization.[5,6] The mechanism of the polymer-forming reactions proceeds *via* nucleophilic aromatic substitution (S_NAr) in which an activated arene monomer substrate, typically an aryl halide, is attacked by a nucleophilic phenoxide.[7] This has traditionally been understood to proceed by the initial formation of a negatively charged σ complex, commonly referred to as a Jackson–Meisenheimer complex, followed by elimination of the halide to form the diaryl ether-containing polymer.[7,8]

Experimental investigations have demonstrated that such Meisenheimer complexes are usually transient but may be formed as stable species during the course of reactions involving the attack of very nucleophilic reagents on very electron-deficient substrates.[9] Mass spectrometry experiments have also demonstrated that stable Meisenheimer complexes may be formed between very electron-deficient benzenes and various nucleophiles in the gas phase.[10]

Previous computational studies on the mechanisms of S_NAr reactions suggest that Meisenheimer complexes may not be formed in a majority of reactions; instead, computed stationary points, thought to be Meisenheimer complexes, may in fact be transition states, not local energy minima on the potential energy surface of the nucleophilic substitution reaction.[11] Other studies suggest that the formation of stable Meisenheimer complex intermediates instead of transition states is dependent on the degree of electron deficiency of the nucleophilic phenoxides in these reactions.[12]

Importantly, none of the cited computational examples surveyed the effect of a coordinating cationic species on the mechanisms for the nucleophilic substitution reaction or examined the likelihood of formation of Meisenheimer complexes over the course of the reaction. Herein we describe computational investigations of ether formation *via* S_NAr reactions of group I metal phenoxides with a series of electron-rich and -deficient halobenzenes. These are models for the formation of commercial polymers such as UDEL

Received: March 19, 2013
Published: May 5, 2013

   dx.doi.org/10.1021/jo400550c | J. Org. Chem. 2013, 78, 5436–5443

polysulfone *via* the base-catalyzed etherification of aryl halides (Scheme 1). We have also examined the displacement of

Scheme 1

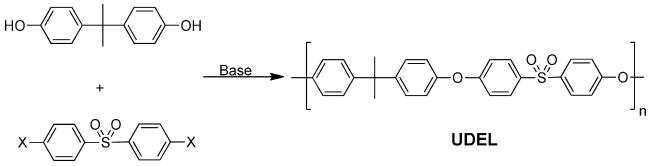

fluoride and nitrite leaving groups to evaluate the effect of these leaving groups in S_NAr reactions of fluorobenzenes and nitrobenzenes.

Our studies reveal that the cationic metal does not speed up the rate of reaction compared with the metal-free anion, but assumes several roles during these mechanisms including binding both reactants and facilitating displacement of the leaving group. These studies have also led to the formulation of a simple computational method to predict reactivity trends in such reactions. These trends have also been rationalized with the distortion/interaction energy model. Importantly, we were also able to evaluate whether Meisenheimer complexes are formed during the course of reactions involving halobenzenes substituted with one or more electron-withdrawing groups. Finally, our studies have revealed that the barrier of the reaction decreases as the size of the metal increases among the series of early group I metal phenoxides. The distortion/interaction energy model has also been used to rationalize this trend.

COMPUTATIONAL METHODS

All calculations were performed with GAMESS-US[13,14] using the dispersion-corrected[15] B3LYP[16−19] density functional theory (DFT) method. Two combinations of basis sets were used in these studies. For most reactions, geometry optimizations were performed with the 6-31+G(d)[20−22] basis set which were followed by single point energy calculations with the aug-cc-pVTZ[23,24] basis set. Geometry optimizations with the VTZP+[25] basis set were also performed for reactions involving a series of group I metal phenoxides. These geometry optimizations were followed by single point energy calculations with the aug-cc-pVTZ basis set applied to all atoms, except for potassium for which the def2-TZVPPD[26,27] basis set was used. A continuum dielectric with the IEF-cPCM[28−31] method was utilized to represent reaction conditions, and all reactions were performed in implicit DMSO solvent. Unless so noted, reported energies are free energies in kcal/mol. Only vibrational free energy corrections to the electronic energy at 298 K were used in accordance with recommendations for molecules optimized in implicit solvent.[32] Normal modes of all structures were examined to verify that ground state structures possess no imaginary frequencies and that one imaginary frequency corresponding to bond formation or bond breaking was obtained for transition structures. Intrinsic reaction coordinate (IRC) calculations were also performed to verify that transition states are connected to reactant complexes and product complexes or Meisenheimer complexes on the potential energy surfaces of reactions.

RESULTS AND DISCUSSION

The experimental protocol for S_NAr polymerizations of phenols with halobenzenes typically requires the presence of the basic salts, K_2CO_3 or Na_2CO_3. It is expected that sodium or potassium phenolates are initially formed by the reaction of the phenol with the base under these conditions. Accordingly, the majority of the work presented herein utilizes reactions between a series of monoactivated *para*-halobenzenes (**1**) with sodium cresolate (**2**) to form diarylethers (**3**) (Scheme 2).

Scheme 2

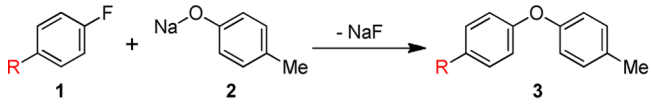

R =
MeO (a), NMe_2 (b)
Me (c), H (d)
F (e), Cl (f)
MeCONH (g), $MeCO_2$ (h)
MeCO (i), $MeSO_2$ (j)
CN (k), NO_2 (l)

The effect of the coordinating metal cation in these reactions was also evaluated by computing ether formation from reactions of lithium, sodium, and potassium cresolates with a selected fluorobenzene.

In addition to studies involving monoactivated *para*-fluorobenzenes, reactions involving arenes substituted at multiple positions with electron-withdrawing groups have also been investigated. These include the reactions of sodium cresolate with the diactivated fluorobenzenes **4**, **5**, and **6** as well as the triactivated fluorobenzenes **7**, **8**, and **9** (Scheme 3).

Scheme 3

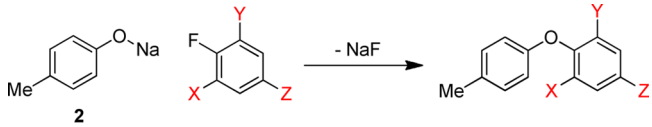

4: X = H, Y = NO_2, Z = SO_2Me
5: X = H, Y = CN, Z = SO_2Me
6: X = H, Y = Z = CN
7: X = Y = NO_2, Z = SO_2Me
8: X = Y = Z = NO_2
9: X = Y = Z = CN

Calculations reveal that the mechanisms of these processes (Scheme 4) involve initial formation of a reactant complex (RC) in which the metal counterion bound to the cresolate also associates with the halobenzene through the halogen atom. The significance of this binding is evident in the subsequent transition state (TS) for S_NAr in which the metal cation facilitates displacement of the halide during nucleophilic attack

Scheme 4

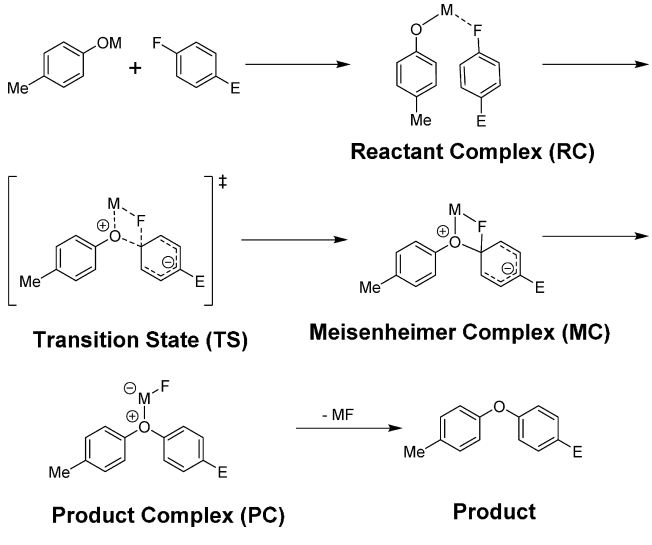

dx.doi.org/10.1021/jo400550c | J. Org. Chem. 2013, 78, 5436−5443

by cresolate. Whether or not Meisenheimer complexes (MCs) are formed after the transition state for S_NAr is dependent on the electron deficiency of the halobenzene. Meisenheimer complexes were not observed when the cresolate is only moderately activated; thus product complexes (PCs) are directly formed from the TS.

Monoactivated *para*-Fluorobenzenes. As illustrated in Figure 1, reaction pathways and free energies for reactions of **2**

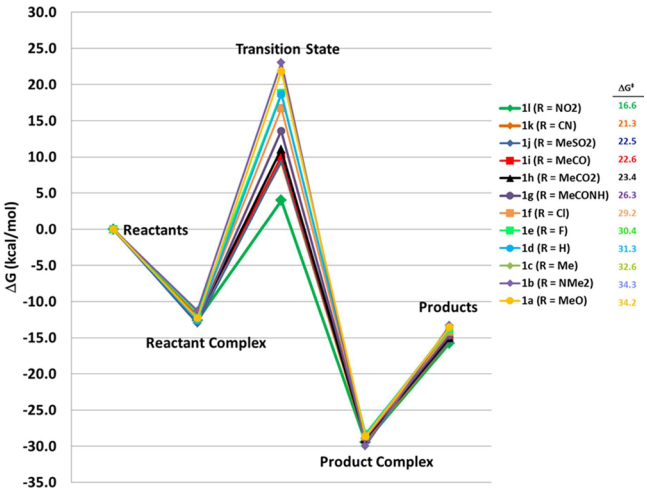

Figure 1. Reaction pathways and free energies for reactions of sodium cresolate, **2**, with the series of *para*-substituted fluorobenzenes, **1**.

with *para*-substituted electron-deficient fluorobenzenes were calculated for a range of electron-deficient arenes. Structures for the reactant complex and transition state of the reaction of **1l** with **2** are shown in Figure 2, demonstrating the binding

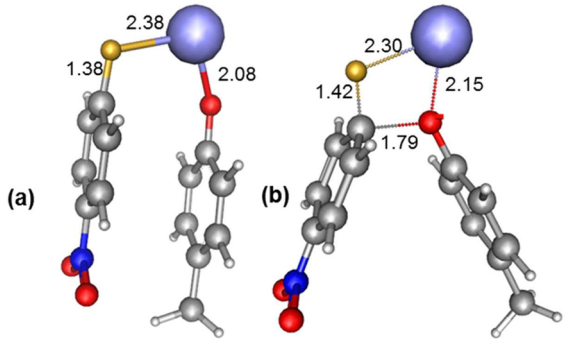

Figure 2. (a) Reactant complex and (b) transition state structure for the reaction of **1l** with **2**. Selected bond distances, in angstrom, are also shown.

exhibited by sodium in both structures. Reactant complexes, RCs, are the minimum-energy structures formed before the transition state, and therefore all barriers are with reference to these stationary points and not to the reactants.

Notably, calculations indicate that Meisenheimer complexes are not formed in these reactions, possibly owing to the fact that the fluorobenzenes are only moderately activated by a single electron-withdrawing group. The parent reaction involving nucleophilic aromatic substitution of fluorobenzene (**1d**) by sodium cresolate possesses a free energy barrier of 31.3 kcal/mol. As expected, fluorobenzene is activated by placement of electron-withdrawing substituents at the *para* position, but electron-donating substituents deactivate fluorobenzene toward electrophilic aromatic substitution. The free energies of activation for reactions involving fluorobenzenes activated by electron-withdrawing substituents **1g**−**1l** are at least 5 kcal/mol lower than the barrier for the parent reaction. The reaction involving the *p*-nitro-substituted fluorobenzene (**1l**) has the lowest barrier, 16.6 kcal/mol, which is ∼4 kcal/mol lower than the next fastest reaction involving the nitrile, **1k**. The amide (**1g**), with a barrier at least ∼3 kcal/mol greater than barriers for other substituents, is the least active electron-withdrawing substituent. Unsurprisingly, barriers for reactions involving **1j**, **1h**, and **1i** (bearing $MeSO_2$-, MeCO-, and $MeCO_2$- substituents in the *para* position, respectively) are all approximately 23 kcal/mol. Reactions involving methoxy- and dimethylamino-substituted fluorobenzenes (**1a** and **1b**, respectively) have the largest barriers, ∼34 kcal/mol, suggesting that the electron-donating ability of these functionalities deactivates the arene toward S_NAr. The activating effect of fluorine at the *para* position (i.e., in 1,4-difluorobenzene, **1e**) is negligible; the barrier of the reaction involving this substrate is 30 kcal/mol, very similar to that of the parent reaction involving fluorobenzene. The reaction involving the displacement of fluorine from 4-chloro-1-fluorobenzene (**1f**) is slightly faster with a barrier of 29 kcal/mol.

Computational Evaluators of Reactivity Trends. Two different approaches have been used to evaluate the activating potency of the substituents in the reactions under investigation. In the first measure, computed free energy barriers for reactions of the *para*-substituted fluorobenzenes with **2** have been correlated with the Löwdin charge[33] on the fluorine-substituted *ipso* carbon atom on the *para*-substituted fluorobenzenes (Figure 3).[34] The charges are well-correlated with the barriers

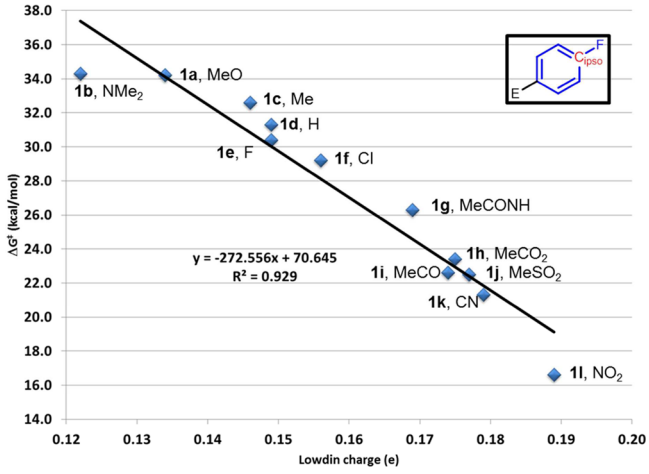

Figure 3. Plot of *e*, Löwdin charge, on the fluorine-substituted *ipso* carbon atom (C_{ipso}) on *para*-substituted fluorobenzenes, **1**, versus free energies of activation for reactions of the *para*-substituted fluorobenzenes, **1**, with sodium cresolate, **2**.

(R^2 = 0.929), suggesting that a computational predictor such as this could be used as a simple diagnostic tool for the prediction of relative reactivities in reactions of *para*-substituted halobenzenes with metal phenolates.

In recent years, a number of groups have demonstrated that reactivity trends for a number of reactions could be assessed by decomposition of activation barriers into two components: the energy required to distort the noninteracting reactants from

dx.doi.org/10.1021/jo400550c | J. Org. Chem. 2013, 78, 5436−5443

their equilibrium geometries into the geometries that they adopt in the transition state; here we term this quantity the distortion energy,[35] E_{dist} (this quantity has also been called the deformation energy[36] and activation strain energy[37]), and the energy gained upon interaction of the distorted reactants at the transition state is termed the interaction energy, E_{int}. Both quantities are related to the activation energy, $E^{‡}$, by the following relationship,

$$E^{‡} = E_{dist} + E_{int} \quad (1)$$

E_{dist} and E_{int} have been computed for the series of reactions of the *para*-substituted fluorobenzenes, **1**, with **2** to gain further insight into the predicted reactivity trends. Shown in Table 1

Table 1. Activation Energies, $E^{‡}$, Interaction Energies, E_{int}, Distortion Energies for Deformed *para*-Substituted Fluorobenzenes, and the Deformed Sodium Cresolate, $E_{dist,1}$ and $E_{dist,2}$, Respectively, and the Total Distortion Energy $E_{dist,total}$ for Reactions of *para*-Substituted Fluorobenzenes with Sodium Cresolate[a]

fluorobenzene	$E^{‡}$	$E_{dist,1}$	$E_{dist,2}$	$E_{dist,total}$	E_{int}	Löwdin charge on **1**
1l	16.5	20.9	2.3	23.2	−6.6	−0.36
1k	21.1	25.6	2.6	28.1	−7.0	−0.33
1j	22.3	26.8	2.5	29.3	−7.0	−0.33
1i	22.7	25.7	2.5	28.1	−5.4	−0.32
1h	23.7	26.7	2.5	29.1	−5.5	−0.33
1g	26.2	28.8	2.5	31.3	−5.1	−0.33
1f	28.8	31.3	2.4	33.7	−4.9	−0.31
1e	30.6	32.9	2.3	35.2	−4.6	−0.29
1d	30.9	32.8	2.3	35.1	−4.2	−0.29
1c	32.6	33.3	2.2	35.6	−2.9	−0.27
1b	33.8	34.8	2.2	36.9	−3.1	−0.27
1a	34.2	33.7	2.2	35.8	−1.6	−0.27

[a]Energies are shown in kcal/mol. Also shown are the sum of Löwdin charges, *e*, on the atoms of fluorobenzene in the transition states.

are the activation energy, $E^{‡}$, the interaction energy, E_{int}, the separate distortion energies of each deformed fluorobenzene, $E_{dist,1}$, and the deformed **2**, $E_{dist,2}$, as well as the total distortion energy $E_{dist,total}$.

Decomposition of the activation energies for these reactions into distortion energies and interaction energies reveals that interaction energies are proportionally much smaller than distortion energies and that the distortion energies for the sodium cresolate reactants in these reactions are also much smaller and are constant across the series of reactions. Consequently, the major component of the energy required to arrive at the transition state involves distortion of the fluorobenzene reactants from their equilibrium geometries into the geometries that they acquire at the transition state. Moreover, there is a signficant degree of correlation (R^2 = 0.944) between $E^{‡}$ and $E_{dist,2}$ as shown in Figure 4.

Close examination of structural features for *para*-substituted arylfluorides in the transition structures of these reactions demonstrates that neither activation energies nor distortion energies are correlated with the length of the C−F bond; neither is there much correlation between barriers and the degree with which the fluorine atom bends out of the plane of the aryl ring (see Supporting Information for details). There is some degree of correlation, however, between the distortion energy of the fluorobenzenes, $E_{dist,2}$, and the Löwdin charge

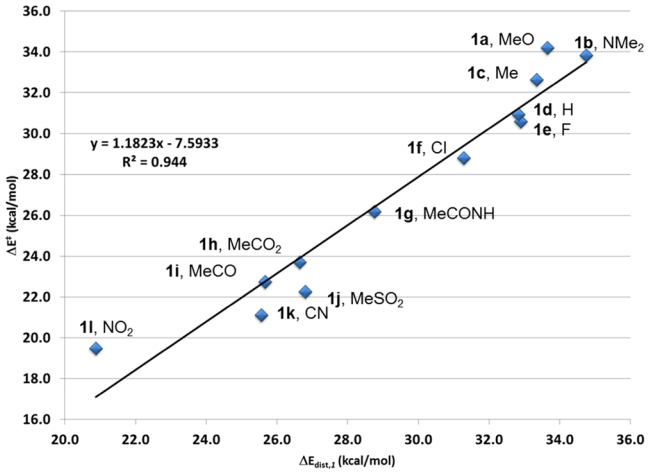

Figure 4. Plot of $E_{dist,1}$, energy required to distort the *para*-substituted fluorobenzenes, **1**, to their transition state geometries versus energies of activation for reactions of *para*-substituted fluorobenzenes with sodium cresolate, **2**.

transferred from the cresolate to the fluorobenzene reactants in the transition state as shown in Table 1. More charge is transferred from the cresolate to electron-withdrawing substituents than to electron-neutral or -donating substituents. Thus, the structural characteristics of the series of arylfluorides are similar upon distortion to arrive at the transition state geometry. However, charge is transferred from sodium cresolate to the distorted arylfluoride upon interaction in the transition state. The amount of charge transferred between the interacting addends is dependent on the electron-withdrawing ability of the substituent on the arylfluoride. Consequently, electron-withdrawing substituents are more capable of stabilizing the transition states leading to lower barriers.

Effect of the Leaving Group. Halides and the nitrite group are typical leaving groups employed for nucleophilic aromatic substitution reactions. Reactions of **2** with 1,4-difluorobenzene, 1,4-dinitrobenzene, and 1-fluoro-4-nitrobenzene (**1e**, **1m**, and **1l**, respectively) have been computed to evaluate the susceptibility of the nitrite and fluoride substituents toward displacement (Scheme 5). In the latter case, displacement of the nitrite and fluoride leaving groups was considered separately. Free energy profiles of all four of the resulting reactions are shown in Figure 5.

Scheme 5

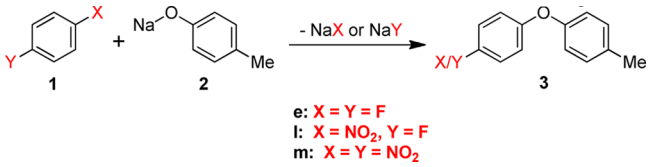

As we previously noted, the fluoride group has a negligible activating effect when stabilizing the negative charge that develops on the aromatic ring in the transition states of these reactions. Thus, the barriers for displacement of the fluoride and nitrite leaving groups in 1,4-difluorobenzene (**1e**) and 1-fluoro-4-nitrobenzene (**1l**), respectively, are 30 and 38 kcal/mol. Notably, the nitrite group is more difficult to displace than the fluoride in this case, partly attributed to the fact that the reactant complex formed from **1l** is more stable than that

dx.doi.org/10.1021/jo400550c | J. Org. Chem. 2013, 78, 5436−5443

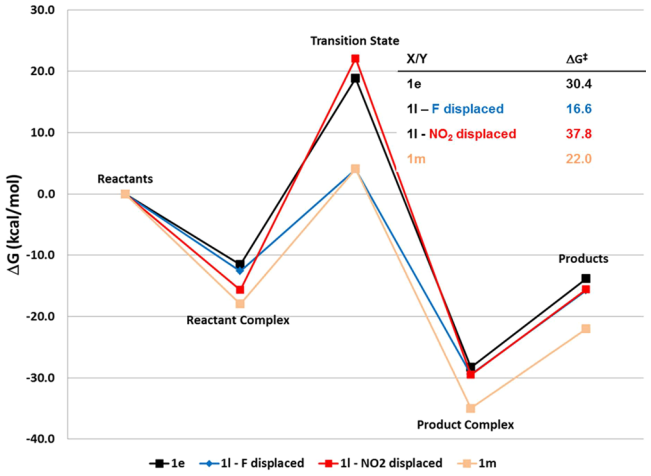

Figure 5. Free energy profiles for the reactions of **1e**, **1l**, and **1m** with sodium cresolate, **2**.

formed by **1e** because of additional stabilization caused by interaction of the nitro group with sodium. The energy of the transition state is also higher with respect to the reactants.

As expected, the nitro group is more proficient than fluorine at stabilizing the developing negative charge in the transition state. Barriers for reactions involving the displacement of nitrite in 1,4-dinitrobenzene (**1m**) and 1-fluoro-4-nitrobenzene (**1l**) are 22 and 17 kcal/mol, respectively. These are at least 8 kcal/mol lower than the displacement of fluoride from corresponding reactions involving 1,4-difluorobenzene and 1-fluoro-4-nitrobenzene (**1e** and **1l**, respectively). The nitrite group in 1,4-dinitrobenzene is more difficult to displace than the fluoride in 1-fluoro-4-nitrobenzene, primarily because the reactant complex formed by 1,4-dinitrobenzene is more strongly stabilized than that formed by 1-fluoro-4-nitrobenzene.

Overall, these results suggest that fluoride is more readily displaced than nitrite in base catalyzed nucleophilic aromatic substitution reactions for the formation of aryl ethers.

Multiply Activated 4-Halobenzenes. Computational investigations were extended to determine how multiple substituents activate fluorobenzenes in nucleophilic aromatic substitution reactions. Thus, reactions of **2** with the disubstituted fluorobenzenes **4**, **5**, and **6** as well as the trisubstituted fluorobenzenes, **7**, **8**, and **9** (Scheme 3) were computed; reaction pathways and energies for these reactions are shown in Figure 6.

Significantly, reactions involving **4** and **6** possess the largest free energies of activation, 15.6 and 13.6 kcal/mol, respectively. The reaction involving the other disubstituted fluorobenzene, **5**, has a much lower barrier. In fact, the barriers for the reaction involving **5** is within ~4 kcal/mol of reactions involving the trisubstituted fluorobenzenes **7**, **8**, and **9**; these reactions all possess barriers lower than 7 kcal/mol, which are at least 13 kcal/mol lower than barriers for reactions involving the monoactivated fluorobenzene analogs **1l**, **1k**, and **1j**. Note that the initial nucleophilic attack is the rate-determining step for reactions involving fluorobenzenes **4**, **5**, **6**, **8**, and **9**. Transition states for breaking the C–F bond (TSCF) present in Meisenheimer complexes are rate-determining for the reaction involving the trisubstituted fluorobenzene **7**.

These studies reveal that Meisenheimer complexes are indeed formed in reactions involving multiply activated fluorobenzenes, as previously found experimentally for reactions involving various nucleophiles.[8−10] The exception is for reactions involving **4** and **6** which, as previously noted, possess much higher barriers than reactions involving multiply activated fluorobenzenes. The enhanced reactivity and the predicted formation of Meisenheimer complexes in reactions involving **5**, **7**, and **8** could be attributed to the fact that these substrates possess nitro subsituents placed *ortho* to the fluorine atom. Due to the proximity of the nitro substituent to sodium, the metal cation is bound to the nitro substituent in the

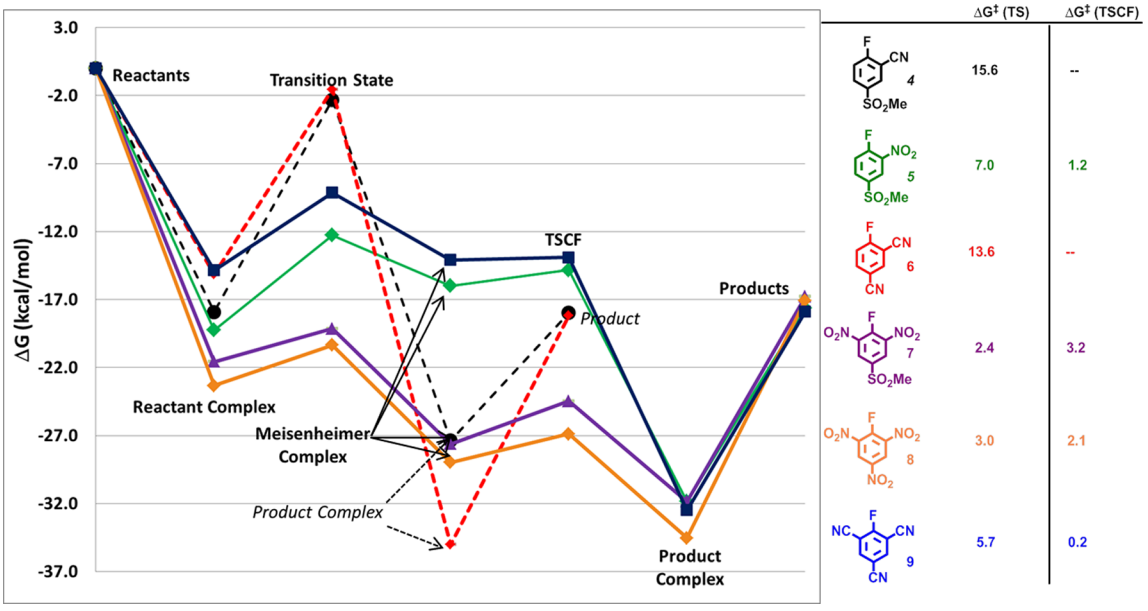

Figure 6. Reaction pathways and free energies for reactions of sodium cresolate with arenes **4**–**9**. Selected stationary points on the pathway for the reaction involving arenes **4** and **6** are shown in italics. $\Delta G^{\ddagger}$ (TS) and $\Delta G^{\ddagger}$ (TSCF) in the accompanying table are with respect to the free energies of the Reactant Complexes and Meisenheimer Complexes, respectively.

dx.doi.org/10.1021/jo400550c | J. Org. Chem. 2013, 78, 5436−5443

transition state for nucleophilic aromatic substitution. This presumably causes the barriers for these reactions to be significantly lowered and stable complexes to be formed after the initial nucleophilic attack. The nitrile substituent, being geometrically linear, lacks the orbital overlap necessary to bind the metal cation, even when it is in an *ortho* position relative to the fluorine atom; thus, the free energies of activation for reactions involving fluorobenzenes **4** and **6** are larger than that for the reaction involving **5**, and no Meisenheimer complexes are formed.

A Meisenheimer complex is formed in the reaction involving the tricyano-substituted fluorobenzene **9**, presumably due to the fact that the fluorobenzene is sufficiently electron-deficient to stabilize the complex, although there is not a great deal of interaction between the metal cation and either of the cyano substituents in the *ortho* position.

Notably, for reactions involving trisubstituted fluorobenzenes, free energy barriers for the formation of product complexes from Meisenheimer complexes via TSCF, the transition state for C–F bond breaking (i.e., the transformation MC → TSCF → PC), are 3 kcal/mol or lower, indicating that the isolation of MCs from these highly activated fluorobenzenes may not be feasible under normal reaction conditions.

These results signify that reaction times for reactions involving *para*-substituted fluorobenzenes can be tremendously accelerated by placing additional activating substituents such as nitro or cyano *ortho* to the fluorine atoms.

Effect of the Coordinating Metal Cation. The effect of the coordinating metal atom was surveyed in two ways. First, reactions of arylfluorides monosubstituted at the *para* position with the NO_2, H, and NMe_2 substituents with the metal-free cresolate anion, **10**, were investigated and compared with reactions involving sodium cresolate, **2**, with the same series of arylfluorides (Figure 7).

As previously explained, all free energies of activation are with respect to the free energies of the low-lying reactant complexes. The free energies of activation for reactions involving the metal-free cresolate anion, **10**, are 10.7, 25.6, and 32.9 kcal/mol for the series of NO_2-, H-, and NMe_2-*para*-substituted arylfluorides; these are lower than corresponding ones involving sodium cresolate, **2**, which have free energies of activation of 16.6, 31.2, and 34.4 kcal/mol, respectively. This difference is primarily caused by the fact that sodium cresolate forms very stable, covalently bound reactant complexes with the arylfluorides, while less stable π-complexes are formed by the interaction of the benzene rings of the cresolate anions with that belonging to the aryl fluorides. These results suggest that free energies of activation are not lowered by the presence of the metal cation.

Very different results are also predicted for the two sets of reactions with regards to the complexes arising from the transition state for nucleophilic attack. For reactions involving aryl-fluorides *para*-substituted with H or NMe_2, the fluoride anion dissociates from the diaryl ether product formed after the transition state. Similar behavior is observed for reactions involving sodium cresolate, **2**, in which the fluorine atom is cleaved from the arylfluoride and product complexes are formed with sodium fluoride bound to the diaryl ether products after the transition state for nucleophilic attack. The notable exception is found for *p*-nitrofluorobenzene, **1l**, in which, interestingly, a Meisenheimer complex is formed with fluoride still covalently bound to the carbon atom of what was once the aryl fluoride. Thus, the presence of the single electron-

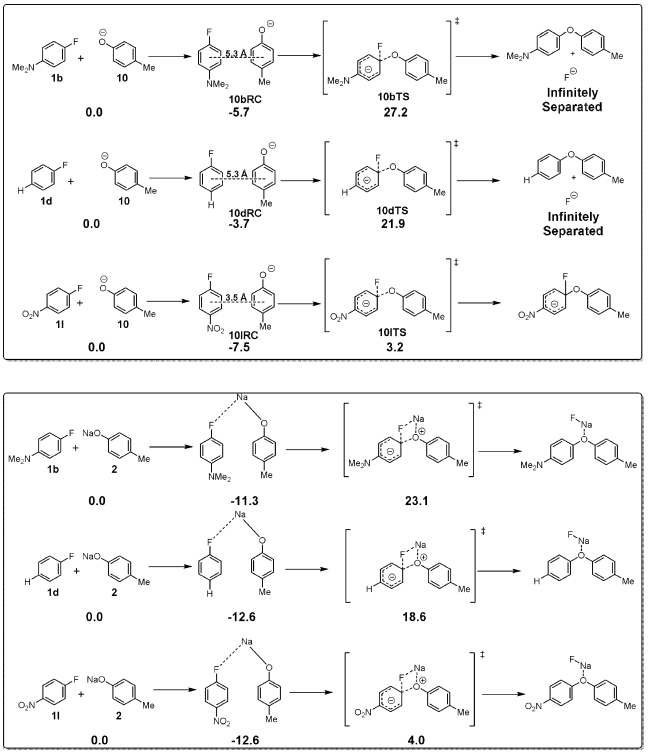

Figure 7. Reactions and free energies for reactions of the cresolate anion, **10**, and of sodium cresolate, **2**, with arylfluorides, **1b**, **1d**, and **1l**.

withdrawing substituent combined with the absence of the sodium ion presumably promotes Meisenheimer complex formation in this moderately activated arylfluoride. Taken together, these results further indicate that the role of the metal cation is to facilitate the binding of arylfluorides during the reaction and to promote displacement of the fluoride from the aryl fluoride.

The series of reactions of group I metal cresolates with methyl 4-fluorobenzoate, **1h** (Scheme 6), were also surveyed in

Scheme 6

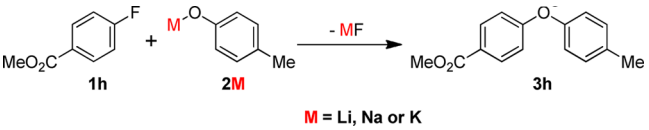

an effort to determine the effects of the type of metal cation used on the energetics of these base-catalyzed reactions. Reaction pathways and free energies for these reactions are shown in Figure 8.

The barriers for reactions involving the lithium, sodium, and potassium cresolates are 25.8, 23.7,[38] and 21.9 kcal/mol. This trend is mainly explained by the fact that, with reference to the free energies of the reactants, the free energies of the transition states decrease in order from lithium cresolate to sodium cresolate to potassium cresolate (14.1 to 11.2 to 10.8, respectively) while the energy of the reactant complexes are only separated by about 1 kcal/mol. This trend could imply that the size of the metal cation influences reactivity: barriers decrease as the size of the metal cation increases.

Further insight was provided by analysis of the distortion and interaction energies for the series of reactions of group I metal cresolates with methyl 4-fluorobenzoate, **1h**, shown in Table 2.

dx.doi.org/10.1021/jo400550c | J. Org. Chem. 2013, 78, 5436–5443

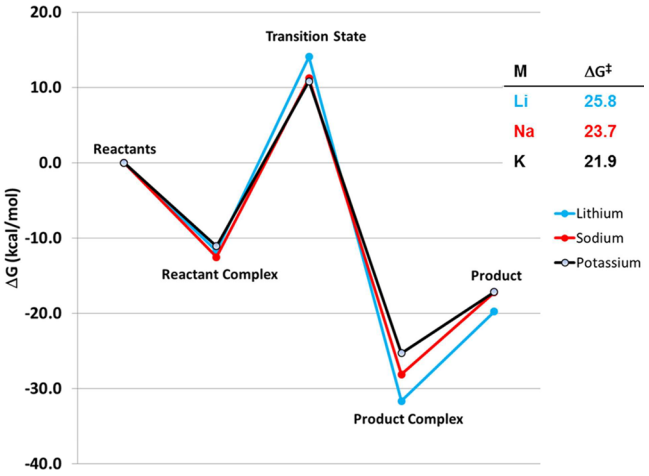

Figure 8. Reaction pathways and free energies for reactions of methyl 4-fluorobenzoate with lithium, sodium, and potassium cresolates.

Table 2. Activation Energies, $E^{\ddagger}$, Interaction Energies, E_{int}, Distortion Energies for *p*-Nitrofluorobenzene, 1h, and the Deformed Sodium Cresolate, $E_{dist,1h}$ and $E_{dist,2M}$, Respectively, and the Total Distortion Energy $E_{dist,total}$ for Reactions of 1h with Sodium Cresolate[a]

metal cation	$E^{\ddagger}$	$E_{dist,1h}$	$E_{dist,2M}$	$E_{dist,total}$	E_{int}
Li	26.2	29.8	3.6	33.3	−7.2
Na	23.8	27.6	2.8	30.4	−6.7
K	21.5	24.2	2.5	26.7	−5.2

[a]All values are in kcal/mol.

These results show that, once again, the energies required to distort the arylfluoride to the transition state geometries, $E_{dist,1h}$, dominate contributions from the distortion energies of the metal cresolates, $E_{dist,2M}$, or interaction energies, E_{int}. Notably, the arylfluoride distortion energies, $E_{dist,1h}$, are correlated with the activation energy, signifying that the lithium cation, being smaller than the other metals, distorts the arylfluoride to a greater degree than the others to arrive at the required geometry for the transition state. In contrast, potassium, the largest cation, does not bind the reactants as closely and, as a consequence, does not distort the arylfluoride as much as the other metals to arrive at the transition state geometry.

CONCLUSION

Calculations with DFT methods have revealed mechanisms and energetics for reactions of metal phenoxides with halobenzenes as models for polyether formation. These calculations have shown that the metal cation binds fluoride or nitrite groups and facilitates removal of these leaving groups during nucleophilic aromatic substitution. However, calculations suggest that the metal does increase the barrier height owing to the stable reactant complexes formed upon binding the arylfluorides. Barriers computed for ether formation from *para*-substituted fluorobenzenes are well correlated with the Löwdin charge of the carbon atom to which the fluorine is attached, a measure of the electron-donating or -withdrawing properties of the substituent at the *para* position. Decomposition of the reaction energies into energies required to distort the reactants into the geometries that they adopt at the transition state as well as energies of the interacting distorted fragments suggest that the dominant component of the barriers are the energies required to distort the arylfluoride reactants. We have found that Meisenheimer complexes are formed in reactions involving very electron-deficient fluorobenzenes, particularly when they contain substituents in the *ortho* position capable of binding with the metal counterion. However, Meisenheimer complexes were not formed in reactions involving fluorobenzenes with a single electron-withdrawing group at the *para* position, suggesting that a Meisenheimer complex cannot be stabilized by placement of a single substituent in the aryl ring where it cannot interact with the metal counterion. Finally, we have found that the barrier to reaction decreases as the size of the metal cation increases among a series of group I metal phenoxides, presumably owing to the fact that the smaller metal cation distorts the phenoxide more than the larger metal cation.

ASSOCIATED CONTENT

Supporting Information

Optimized geometries and free energies; computed free energies at the B3LYP level with the 6-31+G(d), VTZP+, aug-cc-PVTZ, and def2-TZVPPD basis sets. This material is available free of charge via the Internet at http://pubs.acs.org.

AUTHOR INFORMATION

Corresponding Author

*E-mail: hanshorn@us.ibm.com.

Notes

The authors declare no competing financial interest.

REFERENCES

(1) Day, M.; Cooney, J. D.; Wiles, D. M. *J. Appl. Polym. Sci.* **1989**, *38*, 323−327.

(2) Bolt, R. O. Effects of Radiation on Lubricants. In *Handbook of Lubrication and Tribology: Application and Maintenance*; Totten, G. E., Ed.; CRC Press: Boca Raton, FL, 1983; Vol. *1*; Chapter 14. (b) Bolt. R. O., Carroll, J. G., Eds. *Radiation Effects on Organic Materials*; Academic Press: New York, 1963.

(3) Joaquim, M. E. Polyphenyl Ether Lubricants. In *Synthetic Lubricants and High-Performance Functional Fluids*, 2nd ed.; Rudnick, L. R., Shubkin, R. L., Eds.; CRC Press: 1999.

(4) Rose, J. B. In *High Performance Polymers: Their Origin and Development*; Seymour, R. B., Kirshenbaum, G. S., Eds.; Elsevier: New York, 1986; p 187.

(5) (a) Johnson, R. N.; Farnham, A. G.; Clendinning, R. A.; Hale, W. F.; Merriam, C. N. *J. Polym. Sci.: Polym. Chem. Ed.* **1967**, *5*, 2375. (b) Rose, J. B. *Polymer* **1974**, *15*, 456. (c) Attwood, T. E.; Dawson, P. C.; Freeman, J. L.; Hoy, L. R. J.; Rose, J. B.; Staniland, P. A. *Polymer* **1981**, *22*, 1096.

(6) (a) Radlmann, V. E.; Schmidt, W.; Nischk, G. E. *Die Makromol. Chem.* **1969**, *130*, 45. (b) Takekoshi, T.; Wirth, J. G.; Heath, D. R.; Kochanowski, J. E.; Manello, J. S.; Webber, M. J. *J. Polym. Sci.: Polym. Chem. Ed.* **1980**, *18*, 3069. (c) White, D. M.; Takekoshi, T.; Williams, F. J.; Relies, H. M.; Donahue, P. E.; Klopfer, H. J.; Loucks, G. R.; Manello, J. S.; Mathews, R. O.; Schlvenz, R. W. *J. Polym. Sci.: Polym. Chem. Ed.* **1981**, *19*, 16.

(7) Bunnett, J. F.; Zahler, R. E. *Chem. Rev.* **1951**, *49*, 273.

(8) Terrier, F. *Chem. Rev.* **1982**, *82*, 77−152.

(9) Boga, C.; Del Vecchio, E.; Forlani, L.; Mazzanti, A.; Todesco, P. E. *Angew. Chem., Int. Ed.* **2005**, *44*, 3285−3289.

(10) (a) Chiavarino, B.; Crestoni, M. E.; Fornarini, S.; Lanucara, F.; Lemaire, J.; Maître, P. *Angew. Chem., Int. Ed.* **2007**, *46*, 1995−1998. (b) Chen, H.; Chen, H.; Cooks, R. G. *J. Am. Soc. Mass. Spectrom.* **2004**, *15*, 998−1004. (c) Danikiewicz, W.; Bienkowski, T.; Poddebniak, D. *J. Am. Soc. Mass. Spectrom.* **2004**, *15*, 927−933.

(11) (a) Fernández, I.; Frenking, G.; Uggerud, E. *J. Org. Chem.* **2010**, *75*, 2971−2980. (b) Giroldo, T.; Xavier, L. A.; Riveros, J. M. *Angew. Chem., Int. Ed.* **2004**, *43*, 3588−3590.

(12) Glukhotsev, M. N.; Bach, R. D.; Laiter, S. *J. Org. Chem.* **1997**, *62*, 4036−4046.
(13) Schmidt, M. W.; Baldridge, K. K.; Boatz, J. A.; Elbert, S. T.; Gordon, M. S.; Jensen, J. H.; Koseki, S.; Matsunaga, N.; Nguyen, K. A.; Su, S. J.; Windus, T. L.; Dupuis, M.; Montgomery, J. A. *J. Comput. Chem.* **1993**, *14*, 1347−1363.
(14) http://www.msg.ameslab.gov/GAMESS/GAMESS.html (v2010R3).
(15) Grimme, S.; Anthony, J.; Ehrlich, S.; Krieg, H. *J. Chem. Phys.* **2010**, *132*, 154104−154119.
(16) Becke, A. D. *J. Chem. Phys.* **1993**, *98*, 5648−5652.
(17) Lee, C.; Yang, W.; Parr, R. G. *Phys. Rev. B* **1988**, *37*, 785−789.
(18) Vosko, S. H.; Wilk, L.; Nusair, M. *Can. J. Phys.* **1980**, *58*, 1200−1211.
(19) Stephens, P. J.; Devlin, F. J.; Chabalowski, C. F.; Frisch, M. J. *J. Phys. Chem.* **1994**, *98*, 11623−11627.
(20) Hehre, W. J.; Ditchfield, R.; Pople, J. A. *J. Chem. Phys.* **1972**, *56*, 2257−2261.
(21) Hariharan, P. C.; Pople, J. A. *Theor. Chim. Acta* **1973**, *28*, 213−222.
(22) Clark, T.; Chandrasekhar, J.; Spitznagel, G. W.; Schleyer, P. v. R. *J. Comput. Chem.* **1983**, *4*, 294−301.
(23) Woon, D. E.; Dunning, T. H., Jr. *J. Chem. Phys.* **1995**, *103*, 4572−4585.
(24) Kendall, R. A.; Dunning, T. H., Jr.; Harrison, R. J. *J. Chem. Phys.* **1992**, *96*, 6796−6806.
(25) Schafer, A.; Horn, H.; Ahlrichs, R. *J. Chem. Phys.* **1992**, *97*, 2571−2577. Diffuse s,p functions were added via extrapolation.
(26) Rappoport, D.; Furche, F. *J. Chem. Phys.* **2010**, *133*, 134105.
(27) (a) The EMSL Basis Set Library. https://bse.pnl.gov/bse/portal (accessed 2/8/2012). (b) Feller, D. *J. Comput. Chem.* **1996**, *17*, 1571−1586. (c) Schuchardt, K. L.; Didier, B. T.; Elsethagen, T.; Sun, L.; Gurumoorthi, V.; Chase, J.; Li, J.; Windus, T. L. *J. Chem. Inf. Model.* **2007**, *47*, 1045−1052.
(28) Barone, V.; Cossi, M. *J. Phys. Chem. A* **1998**, *102*, 1995−2001.
(29) Cossi, M.; Rega, N.; Scalmani, G.; Barone, V. *J. Comput. Chem.* **2003**, *24*, 669−681.
(30) Miertuš, S.; Scrocco, E.; Tomasi, J. *Chem. Phys.* **1981**, *55*, 117−129.
(31) Cancès, E.; Mennucci, B.; Tomasi, J. *J. Chem. Phys.* **1997**, *107*, 3032−3041.
(32) Ribeiro, R. F.; Marenich, A. V.; Cramer, C. J.; Truhlar, D. G. *J. Phys. Chem. B* **2011**, *115*, 14556−14562.
(33) (a) Löwdin, P.-O. *Adv. Quantum Chem.* **1970**, *5*, 185−199. (b) Cusachs, I. C.; Politzer, P. *Chem. Phys. Lett.* **1968**, *1*, 529.
(34) Löwdin charges are based on structures computed with the 6-31+G(d,p) basis set, while barriers were evaluated with the aug-cc-pVTZ basis set.
(35) (a) Jones, G. O.; Ess, D. H.; Houk, K. N. *Helv. Chim. Acta* **2005**, *88*, 1702−1710. (b) Jones, G. O.; Houk, K. N. *J. Org. Chem.* **2008**, *73*, 1333−1342. (c) Ess, D. H.; Houk, K. N. *J. Am. Chem. Soc.* **2007**, *129*, 10646−10647. (d) Ess, D. H.; Houk, K. N. *J. Am. Chem. Soc.* **2008**, *130*, 10187−10198. (e) Hayden, A. E.; Houk, K. N. *J. Am. Chem. Soc.* **2009**, *131*, 4084−4089. (f) Osuna, S.; Houk, K. N. *Chem.—Eur. J.* **2009**, *15*, 13219−13231. (g) Ess, D. H. *J. Org. Chem.* **2009**, *74*, 1498−1508. (h) Ess, D. H.; Goddard, W. A., III; Periana, R. A. *Organometallics* **2010**, *29*, 6459−6472. (i) Cheong, P. H.-Y.; Paton, R. S.; Bronner, S. M.; Im, G-Y. J.; Garg, N. K.; Houk, K. N. *J. Am. Chem. Soc.* **2010**, *132*, 1267−1269. (j) Paton, R. S.; Kim, S.; Ross, A. G.; Danishefsky, S. J.; Houk, K. N. *Angew. Chem., Int. Ed.* **2011**, *50*, 10366−10368. (k) Black, K.; Liu, P.; Xu, L.; Doubleday, C.; Houk, K. N. *Proc. Natl. Acad. Sci. U.S.A.* **2012**, *109*, 12860−12865. (l) Lopez, S. A.; Houk, K. N. *J. Org. Chem.* **2013**, *78*, 1778−1783.
(36) (a) Kitaura, K.; Morokuma, K. *Int. J. Quantum Chem.* **1976**, *10*, 325. (b) Nagase, S.; Morokuma, K. *J. Am. Chem. Soc.* **1978**, *100*, 1666. (c) Houk, K. N.; Gandour, R. W.; Strozier, R. W.; Rondan, N. G.; Paquette, L. A. *J. Am. Chem. Soc.* **1979**, *101*, 6797. (d) Froese, R. D. J.; Coxon, J. M.; West, S. C.; Morokuma, K. *J. Org. Chem.* **1997**, *62*, 6991. (e) Koga, N.; Ozawa, T.; Morokuma, K. *J. Phys. Org. Chem.* **1990**, *3*, 519. (f) Coxen, J. M.; Grice, S. T.; Maclagan, R. G. A. R.; McDonald, D. Q. *J. Org. Chem.* **1990**, *55*, 3804. (g) Coxon, J. M.; Rroese, R. D. J.; Ganguly, B.; Marchand, A. P.; Morokuma, K. *Synnlett* **1999**, *11*, 1681. (h) Avalos, M.; Babiano, R.; Bravo, J. L.; Cintas, P.; Jiménez, J.; Palacios, J.; Silva, M. A. *J. Org. Chem.* **2000**, *65*, 6613. (i) Geetha, K.; Dinadayalane, T. C.; Sastry, G. N. *J. Phys. Org. Chem.* **2003**, *16*, 298. (j) Manoharan, M.; Venuvanalingam, P. *J. Chem. Soc., Perkin Trans. 2* **1997**, 1799. (k) Kavitha, K.; Manoharan, M.; Venuvanalingam, P. *J. Org. Chem.* **2005**, *70*, 2528. (l) Kavitha, K.; Venuvanalingam, P. *Int. J. Quantum Chem.* **2005**, *104*, 67. (m) Blowers, P.; Ford, L.; Masel, R. *J. Phys. Chem. A* **1998**, *102*, 9267.
(37) (a) Bickelhaupt, F. M. *J. Comput. Chem.* **1999**, *20*, 114. (b) Velde, G. T.; Bickelhaupt, F. M.; Baerends, E. J.; Guerra, C. F.; Gisbergen, S. J. A. V.; Snijders, J. G.; Ziegler, T. *J. Comput. Chem.* **2001**, *22*, 931. (c) Diefenbach, A.; Bickelhaupt, F. M. *J. Chem. Phys.* **2001**, *115*, 4030. (d) Diefenbach, A.; Bickelhaupt, F. M. *J. Phys. Chem. A* **2004**, *108*, 8460. (e) Diefenbach, A.; Bickelhaupt, F. M. *J. Organomet. Chem.* **2005**, *690*, 2191. (f) Diefenbach, A.; de Jong, G. T.; Bickelhaupt, F. M. *Mol. Phys.* **2005**, *103*, 995. (g) Diefenbach, A.; de Jong, G. T.; Bickelhaupt, F. M. *J. Chem. Theory Comput.* **2005**, *1*, 286. (h) Stralen, J. N. P.v.; Bickelhaupt, F. M. *Organometallics* **2006**, *25*, 4260. (i) de Jong, G. T.; Visser, R.; Bickelhaupt, F. M. *J. Organomet. Chem.* **2006**, *691*, 4341. (j) de Jong, G. T.; Bickelhaupt, F. M. *Chem. Phys. Chem.* **2007**, *8*, 1170. (k) de Jong, G. T.; Bickelhaupt, F. M. *J. Chem. Theory Comput.* **2007**, *3*, 514.
(38) The free energy barriers for the reaction of sodium cresolate with methyl 4-fluorobenzoate calculated with the B3LYP-D3/aug-cc-pVTZ//B3LYP-D3/VTZP+ and B3LYP-D3/aug-cc-pVTZ//B3LYP-D3/6-31+G(d,p) methods are almost identical, 23.7 and 23.4 kcal/mol, respectively.